Chapter 6

A Unified Accurate Solution for Three-dimensional Vibration Analysis of Functionally Graded Plates and Cylindrical Shells with General Boundary Conditions

Guoyong Jin, Zhu Su and Tiangui Ye

Additional information is available at the end of the chapter

http://dx.doi.org/10.5772/62335

Abstract

Three-dimensional (3-D) vibration analysis of thick functionally graded plates and cylindrical shells with arbitrary boundary conditions is presented in this chapter. The effective material properties of functionally graded structures vary continuously in the thickness direction according to the simple power-law distributions in terms of volume fraction of constituents and are estimated by Voigt's rule of mixture. By using the artificial spring boundary technique, the general boundary conditions can be obtained by setting proper spring stiffness. All displacements of the functionally graded plates and shells are expanded in the form of the linear superposition of standard 3-D cosine series and several supplementary functions, which are introduced to remove potential discontinuity problems with the original displacements along the edge. The Rayleigh-Ritz procedure is used to yield the accurate solutions. The convergence, accuracy and reliability of the current formulation are verified by numerical examples and by comparing the current results with those in published literature. Furthermore, the influence of the geometrical parameters and elastic foundation on the frequencies of rectangular plates and cylindrical shells is investigated.

Keywords: Three-dimensional elasticity theory, functional graded materials, plate and cylindrical shell, general boundary conditions

1. Introduction

Functionally graded materials (FGMs) are a new type of composite materials with smooth and continuous variation in material properties in desired directions. This is achieved by gradually varying the volume fraction of the constituent materials. Such materials possess various advantages over conventional composite laminates, such as smaller stress concentration,

higher fracture toughness and improved residual stress distribution. Recently, the FGMs have been used to build plate and shell components in various engineering applications, especially mechanical, aerospace, marine and civil engineering. In some cases, those FGM plates and shells are frequently subjected to dynamic loads, which leads to the vibration behaviours, which may cause fatigue damage and result in severe reduction in the strength and stability of the whole structures. Therefore, the vibration analysis of the FGM plates and shells is required and it is important to provide insight into dynamic behaviours and optimal design.

It is well known that vibration problems deal with two main concepts: plate and shell theories and computational approaches. The development of plate and shell theories has been subjected to significant research interest for many years, and many plate and shell theories have been proposed and developed. The main plate and shell theories can be classified into two categories: two-dimensional (2-D) plate and shell theories, including classic plate and shell theory (CPT) [1–4], the first-order shear deformation theory (FSDT) [5–16], and the higher order shear deformation theory (HSDT) [17–26], and three-dimensional (3-D) theory of elasticity [27–35]. However, all 2-D theories are approximate because they were developed based on certain kinematic assumptions that result in relatively simple expression and derivation of solutions. Actually, 3-D elasticity theory, which does not rely on any hypotheses about the distribution field of deformations and stress, not only provides realistic results but also allows for further physical insight. More attempts have been made for 3-D vibration analysis of plates and shells in the recent decades. Furthermore, many analytical, semi-analytical and numerical computational methods have also been developed, such as Ritz method, state-space method, differential quadrature method (DQM), Galerkin method, meshless method, finite element method (FEM) and discrete singular convolution (DSC) approach.

However, a close scrutiny of the literature in this field reveals that most investigations were carried out based on 2-D plate and shell theories, and a general 3-D solution for this subject seems to be limited. Moreover, the review also reveals that most of previous research efforts were restricted to vibration problems of FGM plates and shells with limited sets of classical boundary conditions. It is well recognized that there exist various possible boundary restraint cases for plates and shells in practical assembly and engineering applications. Consequently, it is necessary and of great significance to develop a unified, efficient and accurate method that is capable of universally dealing with FGM plates and shells with general boundary conditions.

In view of these apparent voids, the aim of this chapter is to develop an accurate semi-analysis method that is capable of dealing with vibrations of FGM plates and shells with general boundary conditions, including classical boundaries, elastic supports and their combinations and to provide a summary of known 3-D results of plates and shells with general boundary conditions, which may serve as benchmark solutions for future researches in this field.

In this chapter, 3-D vibration analysis of thick functionally graded plates and cylindrical shells with arbitrary elastic restraints is presented. The effective material properties of functionally graded structures vary continuously in the thickness direction according to the simple power-law distributions in terms of volume fraction of constituents and are estimated by Voigt's rule

http://dx.doi.org/10.5772/62335

of mixture. By using the artificial spring boundary technique, the general boundary conditions can be obtained by setting proper spring stiffness. All displacements of the functionally graded plates and shells are expanded in the form of the linear superposition of standard 3-D cosine series and several supplementary functions, which are introduced to remove potential discontinuity problems with the original displacements along the edge. The RayleighRitz procedure is used to yield the accurate solutions.

2. Theoretical formulations

2.1. Preliminaries

A differential element of a shell with uniform thickness h is considered, as shown in Fig. 1. An orthogonal curvilinear coordinate system composed of coordinates α, β and z coordinates is located on the bottom surface. The u, v and w denote the displacement components of an arbitrary point in the α, β and z directions, respectively. Within the context of 3-D elasticity theory, the linear strain-displacement relations can be expressed as follows [36]:

$$\varepsilon_{\alpha\alpha} = \frac{1}{h_\alpha}\frac{\partial u}{\partial \alpha} + \frac{1}{h_\alpha h_\beta}\frac{\partial h_\alpha}{\partial \beta}v + \frac{1}{h_\alpha h_z}\frac{\partial h_\alpha}{\partial z}w \tag{1}$$

$$\varepsilon_{\beta\beta} = \frac{1}{h_\beta}\frac{\partial v}{\partial \beta} + \frac{1}{h_\beta h_z}\frac{\partial h_\beta}{\partial z}w + \frac{1}{h_\beta h_\alpha}\frac{\partial h_\beta}{\partial \alpha}u \tag{2}$$

$$\varepsilon_{zz} = \frac{1}{h_z}\frac{\partial w}{\partial z} + \frac{1}{h_z h_\alpha}\frac{\partial h_z}{\partial \alpha}u + \frac{1}{h_z h_\beta}\frac{\partial h_z}{\partial \beta}v \tag{3}$$

$$\gamma_{\beta z} = \frac{1}{h_\beta h_z}\left(h_\beta \frac{\partial v}{\partial z} + h_z \frac{\partial w}{\partial \beta} - \frac{\partial h_\beta}{\partial z}v - \frac{\partial h_z}{\partial \beta}w\right) \tag{4}$$

$$\gamma_{\alpha z} = \frac{1}{h_\alpha h_z}\left(h_\alpha \frac{\partial u}{\partial z} + h_z \frac{\partial w}{\partial \alpha} - \frac{\partial h_\alpha}{\partial z}u - \frac{\partial h_z}{\partial \alpha}w\right) \tag{5}$$

$$\gamma_{\alpha\beta} = \frac{1}{h_\alpha h_\beta}\left(h_\alpha \frac{\partial u}{\partial \beta} + h_\beta \frac{\partial v}{\partial \alpha} - \frac{\partial h_\beta}{\partial \alpha}v - \frac{\partial h_\alpha}{\partial \beta}u\right) \tag{6}$$

where ε_α, ε_β, ε_z, $\varepsilon_{\beta z}$, $\varepsilon_{\alpha z}$ and $\varepsilon_{\alpha\beta}$ are the normal and shear strain components, and h_α, h_β and h_z are Lame coefficients.

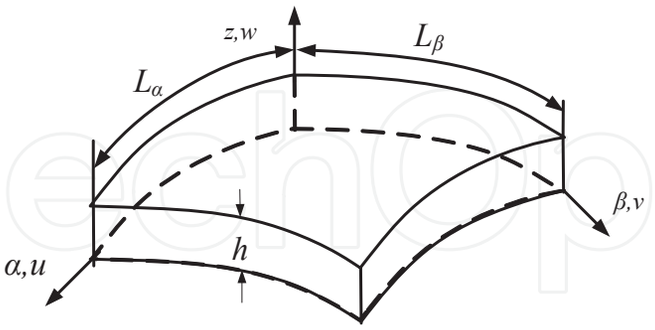

Figure 1. Geometry of differential element of shells

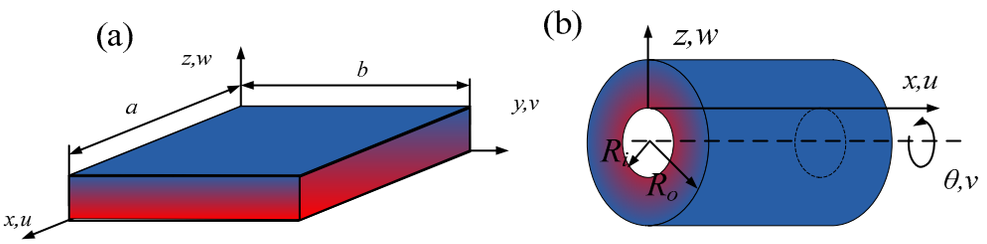

Figure 2. Definition of coordinate systems: (a) plate and (b) cylindrical shell.

In engineering applications, plates and shells are the basic structural elements. For the sake of brevity, this chapter will be confined to rectangular plates and cylindrical shells. According to Fig. 2, the coordinate systems and Lame coefficients are given as follows [36]: for rectangular plates, $\alpha=x$, $\beta=y$, $z=z$, $h_\alpha=h_\beta=h_\gamma=1$ and for cylindrical shells, $\alpha=x$, $\beta=\theta$, $z=r$, $h_\alpha=h_\gamma=1$, $h_\beta=R_i+r$. The explicit expressions of strains can be obtained by substituting above quantities into Eqs. (1–6). The 3-D linear constitutive relations for the plates and shells can be written as follows:

$$\begin{bmatrix}\sigma_{\alpha\alpha}\\ \sigma_{\beta\beta}\\ \sigma_{zz}\\ \sigma_{\beta z}\\ \sigma_{\alpha z}\\ \sigma_{\alpha\beta}\end{bmatrix}=\begin{bmatrix}Q_{11} & Q_{12} & Q_{13} & 0 & 0 & 0\\ Q_{12} & Q_{22} & Q_{23} & 0 & 0 & 0\\ Q_{13} & Q_{23} & Q_{33} & 0 & 0 & 0\\ 0 & 0 & 0 & Q_{44} & 0 & 0\\ 0 & 0 & 0 & 0 & Q_{55} & 0\\ 0 & 0 & 0 & 0 & 0 & Q_{66}\end{bmatrix}\begin{bmatrix}\varepsilon_{\alpha\alpha}\\ \varepsilon_{\beta\beta}\\ \varepsilon_{zz}\\ \gamma_{\beta z}\\ \gamma_{\alpha z}\\ \gamma_{\alpha\beta}\end{bmatrix} \tag{7}$$

where Q_{ij} (i, j = 1–6) are the elastic coefficients and are given as:

http://dx.doi.org/10.5772/62335

$$
\begin{aligned}
Q_{11} = Q_{22} = Q_{33} &= \frac{E(r)[1-\mu(r)]}{[1+\mu(r)][1-2\mu(r)]}, \\
Q_{12} = Q_{13} = Q_{23} &= \frac{\mu(r)E(r)}{[1+\mu(r)][1-2\mu(r)]}, \\
Q_{44} = Q_{55} = Q_{66} &= \frac{E(r)}{[2(1+\mu(r)]},
\end{aligned} \tag{8}
$$

where $E(r)$ and $\mu(r)$ are the effective Young's modulus and Poisson's ratio of a FGMs, respectively. In this chapter, it is assumed that the FGMs are manufactured by ceramic and metallic constituents, and the effective material properties of FGMs can be expressed as follows [37]:

$$
\begin{aligned}
E(r) &= (E_c - E_m)V_c + E_m \\
\mu(r) &= (\mu_c - \mu_m)V_c + \mu_m \\
\rho(r) &= (\rho_c - \rho_m)V_c + \rho_m
\end{aligned} \tag{9}
$$

where E, μ, ρ and V are Young's modulus, Poisson's ratio, density and volume fraction, respectively. The subscripts c and m donate the ceramic and metallic constituents, respectively. The ceramic volume fraction follows simple power-law distribution:

$$
V_c = (\frac{z}{h})^p, V_m = 1 - (\frac{z}{h})^p \qquad (0 \le z \le h) \tag{10}
$$

where z is the thickness coordinate, and p is the power-law index that takes only positive values. The value of p equal to zero represents a fully ceramic plate, whereas infinite p indicates a fully metallic plate.

In this work, the general boundary conditions can be described in terms of three groups of springs (k_u, k_v, k_w). Taking edge α = constant, for example, the boundary conditions can be given as follows:

$$
k_u^{\alpha 1} u = \sigma_{\alpha\alpha}, k_v^{\alpha 1} v = \sigma_{\alpha\beta}, k_w^{\alpha 1} w = \sigma_{\alpha z} \tag{11}
$$

$$
k_u^{\alpha 2} u = \sigma_{\alpha\alpha}, k_v^{\alpha 2} v = \sigma_{\alpha\beta}, k_w^{\alpha 2} w = \sigma_{\alpha z} \tag{12}
$$

where the superscripts $\alpha 1$ and $\alpha 2$ denote the edges of $\alpha = 0$ and $\alpha = L_1$, respectively. For the rectangular plates, the similar conditions exist for the edges of β = constant. The classical boundary conditions and elastic restrains can be obtained by easily changing the values of boundary spring.

2.2. Energy functional

The energy functional of plates or shells can be expressed as follows:

$$\Pi = T - U - P \tag{13}$$

where T is kinetic energy, U is elastic strain energy, and P denotes the potential energy stored in boundary springs.

The kinetic energy T can be written as follows:

$$T = \frac{1}{2}\iiint \rho(z)\left(\dot{u}^2 + \dot{v}^2 + \dot{w}^2\right)\mathrm{d}\alpha\mathrm{d}\beta\mathrm{d}z \tag{14}$$

where the over dot represents the differentiation with respect to time.

The strain energy U can be written in an integral form as follows:

$$U = \frac{1}{2}\iiint\left(\sigma_{\alpha\alpha}\varepsilon_{\alpha\alpha} + \sigma_{\beta\beta}\varepsilon_{\beta\beta} + \sigma_{zz}\varepsilon_{zz} + \sigma_{\beta z}\gamma_{\beta z} + \sigma_{\alpha z}\gamma_{\alpha z} + \sigma_{\alpha\beta}\gamma_{\alpha\beta}\right)\mathrm{d}\alpha\mathrm{d}\beta\mathrm{d}z \tag{15}$$

Substituting Eqs. (1–16) into Eq. (15) together with Lame coefficients, one can obtain the explicit expressions of strain energy for rectangular plates and cylindrical shells.

The potential energy (P) stored in the boundary springs is given as follows:

$$P = \frac{1}{2}\left[\int_{S_{\alpha i}}\left(k_u^{\alpha i}u^2 + k_v^{\alpha i}v^2 + k_w^{\alpha i}w^2\right)\mathrm{d}S_{\alpha i} + \int_{S_{\beta i}}\left(k_u^{\beta i}u^2 + k_v^{\beta i}v^2 + k_w^{\beta i}w^2\right)\mathrm{d}S_{\beta i}\right] \tag{16}$$

where $S_{\alpha i}$ and $S_{\beta i}$ denote the area of boundary surfaces.

2.3. Admissible functions

It is crucially important to construct the appropriate admissible displacement functions in the Rayleigh–Ritz method. Beam functions, orthogonal polynomials and Fourier series are often used as displacement functions of plates and shells. However, the use of beam function will lead to at least a very tedious solution process [38]. The problem with using a complete set of orthogonal polynomials is that the higher-order polynomials tend to become numerically unstable because of the computer round-off errors [38, 39]. These numerical difficulties can be avoided by the Fourier series because the Fourier series constitute a complete set and exhibit an excellent numerical stability. However, when the displacements are expressed in terms of conventional Fourier series, discontinuities potentially exist in the original displacements and

http://dx.doi.org/10.5772/62335

their derivatives. In this chapter, a modified Fourier series defined as the linear superposition of a 3-D Fourier cosine series and some auxiliary polynomial functions is used to express the displacement components, which are given as follows [40–43]:

$$u(\alpha,\beta,z,t)=\left\{\begin{array}{l}\sum_{m=0}^{M}\sum_{n=0}^{N}\sum_{q=0}^{Q}A_{mnq}\cos\lambda_m\alpha\cos\lambda_n\beta\cos\lambda_q z+\\ \sum_{l=1}^{2}\sum_{n=0}^{N}\sum_{q=0}^{Q}a_{lnq}\xi_{l\alpha}(\alpha)\cos\lambda_n\beta\cos\lambda_q z+\\ \sum_{m=0}^{M}\sum_{l=1}^{2}\sum_{q=0}^{Q}\bar{a}_{lmq}\cos\lambda_m\alpha\xi_{l\beta}(\beta)\cos\lambda_q z+\\ \sum_{m=0}^{M}\sum_{n=0}^{N}\sum_{l=1}^{2}\tilde{a}_{lmn}\cos\lambda_m\alpha\cos\lambda_n\beta\xi_{lz}(z)+\end{array}\right\}e^{j\omega t} \tag{17}$$

$$v(\alpha,\beta,z,t)=\left\{\begin{array}{l}\sum_{m=0}^{M}\sum_{n=0}^{N}\sum_{q=0}^{Q}B_{mnq}\cos\lambda_m\alpha\cos\lambda_n\beta\cos\lambda_q z+\\ \sum_{l=1}^{2}\sum_{n=0}^{N}\sum_{q=0}^{Q}b_{lnq}\xi_{l\alpha}(\alpha)\cos\lambda_n\beta\cos\lambda_q z+\\ \sum_{m=0}^{M}\sum_{l=1}^{2}\sum_{q=0}^{Q}\bar{b}_{lmq}\cos\lambda_m\alpha\xi_{l\beta}(\beta)\cos\lambda_q z+\\ \sum_{m=0}^{M}\sum_{n=0}^{N}\sum_{l=1}^{2}\tilde{b}_{lmn}\cos\lambda_m\alpha\cos\lambda_n\beta\xi_{lz}(z)+\end{array}\right\}e^{j\omega t} \tag{18}$$

$$w(\alpha,\beta,z,t)=\left\{\begin{array}{l}\sum_{m=0}^{M}\sum_{n=0}^{N}\sum_{q=0}^{Q}C_{mnq}\cos\lambda_m\alpha\cos\lambda_n\beta\cos\lambda_q z+\\ \sum_{l=1}^{2}\sum_{n=0}^{N}\sum_{q=0}^{Q}c_{lnq}\xi_{l\alpha}(\alpha)\cos\lambda_n\beta\cos\lambda_q z+\\ \sum_{m=0}^{M}\sum_{l=1}^{2}\sum_{q=0}^{Q}\bar{c}_{lmq}\cos\lambda_m\alpha\xi_{l\beta}(\beta)\cos\lambda_q z+\\ \sum_{m=0}^{M}\sum_{n=0}^{N}\sum_{l=1}^{2}\tilde{c}_{lmn}\cos\lambda_m\alpha\cos\lambda_n\beta\xi_{lz}(z)+\end{array}\right\}e^{j\omega t} \tag{19}$$

where $\lambda_m=m\pi/L_\alpha$, $\lambda_n=n\pi/L_\beta$, $\lambda_q=q\pi/L_z$. A_{mnq}, a_{lnq}, $\bar{a}_{lmq}$, $\tilde{a}_{lmn}$, B_{mnq}, b_{lnq}, $\bar{b}_{lmq}$, $\tilde{b}_{lmn}$, C_{mnq}, c_{lnq}, $\bar{c}_{lmq}$ and $\tilde{c}_{lmn}$ are the unknown coefficients that need to be determined in future. ω is the circular frequency and t is the time variable. $\xi_{l\alpha}$, $\xi_{l\beta}$ and ξ_{lz} represent a set of closed-form sufficiently smooth functions introduced to remove the discontinuities of the original displacement functions and their derivatives at edges and then to accelerate the convergence of the series representations. According to the 3-D elasticity theory, it is required that at least two-order

derivatives of the displacement functions exist and continuous at any point. Consequently, two auxiliary functions in every direction are supplemented, as shown in Eqs. (17–19). The auxiliary functions are given as follows:

$$\xi_{1\alpha} = \alpha\left(\frac{\alpha}{L_\alpha} - 1\right)^2, \xi_{2\alpha} = \frac{\alpha^2}{L_\alpha}\left(\frac{\alpha}{L_\alpha} - 1\right) \tag{20}$$

$$\xi_{1\beta} = \beta\left(\frac{\beta}{L_\beta} - 1\right)^2, \xi_{2\beta} = \frac{\beta^2}{L_\beta}\left(\frac{\beta}{L_\beta} - 1\right) \tag{21}$$

$$\xi_{1z} = z\left(\frac{z}{L_z} - 1\right)^2, \xi_{2z} = \frac{z^2}{L_z}\left(\frac{z}{L_z} - 1\right) \tag{22}$$

It is easy to verify that

$$\xi_{1\alpha}(0) = \xi_{1\alpha}(L_\alpha) = \xi'_{1\alpha}(L_\alpha) = 0,\ \xi'_{1\alpha}(0) = 1 \tag{23}$$

$$\xi_{2\alpha}(0) = \xi_{2\alpha}(L_\alpha) = \xi'_{2\alpha}(0) = 0,\ \xi'_{2\alpha}(L_\alpha) = 1 \tag{24}$$

The similar conditions exist for the β- and z-related polynomials. It should be mentioned that as the circumferential symmetry of the cylindrical shells in the coordinate θ, the 3-D problem of the cylindrical shell can be transformed to 2-D analysis by using the Fourier series in circumferential direction.

2.4. Solution procedure

Substituting Eqs. (14–16) into Eq. (13) together with the displacement functions defined in Eqs. (17–19) and performing the Rayleigh–Ritz operation, a set of linear algebraic equation against the unknown coefficients can be obtained as follows:

$$\left\{\mathbf{K} - \omega^2\mathbf{M}\right\}\mathbf{X} = \mathbf{0} \tag{25}$$

where $\mathbf{K}$ is the total stiffness matrix for the structure and $\mathbf{M}$ is the total mass matrix. Both of them are symmetric matrices. $\mathbf{X}$ is the column matrix composed of unknown coefficients expressed in the following form:

$$\mathbf{X} = [\mathbf{X}_u, \mathbf{X}_v, \mathbf{X}_w]^T \tag{26}$$

where

$$\mathbf{X}_u = \begin{Bmatrix} A_{000}, \cdots, A_{mnq}, \cdots, A_{MNQ}, a_{100}, \cdots, a_{lnq}, \cdots, a_{2NQ}, \\ \overline{a}_{100}, \cdots, \overline{a}_{lmq}, \cdots \overline{a}_{2MQ}, \tilde{a}_{100}, \cdots, \tilde{a}_{lmn}, \cdots \tilde{a}_{2MN} \end{Bmatrix} \tag{27}$$

$$\mathbf{X}_v = \begin{Bmatrix} B_{000}, \cdots, B_{mnq}, \cdots, B_{MNQ}, b_{100}, \cdots, b_{lnq}, \cdots, b_{2NQ}, \\ \overline{b}_{100}, \cdots, \overline{b}_{lmq}, \cdots \overline{b}_{2MQ}, \tilde{b}_{100}, \cdots, \tilde{b}_{lmn}, \cdots \tilde{b}_{2MN} \end{Bmatrix} \tag{28}$$

$$\mathbf{X}_w = \begin{Bmatrix} C_{000}, \cdots, C_{mnq}, \cdots, C_{MNQ}, c_{100}, \cdots, c_{lnq}, \cdots, c_{2NQ}, \\ \overline{c}_{100}, \cdots, \overline{c}_{lmq}, \cdots \overline{c}_{2MQ}, \tilde{c}_{100}, \cdots, \tilde{c}_{lmn}, \cdots \tilde{c}_{2MN} \end{Bmatrix} \tag{29}$$

The frequencies can be determined by solving Eq. (25) via the eigenfunction of MATLAB program. The mode shape corresponding to each frequency can be obtained by back substituting the eigenvector to the displacement functions in Eqs. (17–19).

3. Numerical examples and discussion

In this section, several vibration results of FGM plates and cylindrical shells with general boundary conditions are presented to illustrate the accuracy and reliability of the current formulation. To simplify presentation, C, S, F and E denote the clamped, simply supported, free and elastic restraints. Three types of elastic boundary conditions designated by symbols E_1, E_2 and E_3 are considered. E_1-type edge is considered to be elastic in normal direction; the support type E_2 only allows elastically restrained displacement in both tangential directions; when all of three displacements along the edges are elastically restrained, the edge support is defined by E_3. The expressions of the different boundary conditions along the edge $\alpha = 0$ are given as follows:

Free boundary condition (F):

$$\sigma_{\alpha\alpha} = \sigma_{\alpha\beta} = \sigma_{\alpha z} = 0$$

Clamped boundary condition (C):

$$u = v = w = 0$$

Simply supported boundary condition (S):

$$\sigma_{\alpha\alpha} = v = w = 0$$

First type of elastic restraint (E_1):

$$u \neq 0, v = w = 0$$

Second type of elastic restraint (E_1):

$$u = 0, v \neq 0, w \neq 0$$

Three type of elastic restraint (E_1):

$$u \neq 0, v \neq 0, w \neq 0$$

A simple letter is used to describe the boundary conditions of structure. For example, SFCE denotes a plate having simply supported boundary condition at $\alpha = 0$, free boundary condition at $\beta = 0$, clamped boundary condition at $\alpha = L_\alpha$, and elastic restraint at $\beta = L_\beta$; CS denotes a cylindrical shell having clamped boundary condition at $\alpha = 0$ and simply supported boundary condition at $\alpha = L_\alpha$.

3.1. Rectangular plates

In this section, several numerical examples concerning the free vibration of FGM rectangular plates with different geometrical parameters and boundary conditions have been investigated to verify the convergence, accuracy and reliability of the present method. Some new vibration results of rectangular plates with elastic boundary conditions are given. Unless stated otherwise, the material properties for ceramic and metallic constituents of FGM plates are given as follows: $E_c = 380$ GPa, $\mu_c = 0.3$ and $\rho_c = 3800$ kg/m^3 and $E_m = 70$ GPa, $\mu_m = 0.3$ and $\rho_m = 2702$ kg/m^3.

3.1.1. Convergence study

Theoretically, there are infinite terms in the modified Fourier series solution. However, the series is numerically truncated, and only finite terms are counted in actual calculations. The convergence of this method will be checked. Table 1 presents the first seven frequency parameters Ω of completely free FGM square plates. The frequency parameter Ω is defined as follows:

$$\Omega = \omega a^2 / h\sqrt{\rho_c / E_c}$$

http://dx.doi.org/10.5772/62335

The geometrical parameters are given as follows: $a/b = 1$ and $h/b = 0.1$, 0.2 and 0.5. The power-law index p is taken to be $p = 1$. It is obvious that the results of this study show a monotonic trend, and the solutions converge quite rapidly as the truncated number increases. In the following examples, the truncated numbers of the displacement expressions will be uniformly selected as $M \times N \times Q = 13 \times 13 \times 8$.

h/b	$M \times N \times Q$	Ω_1	Ω_2	Ω_3	Ω_4	Ω_5	Ω_6	Ω_7
0.1	9 × 9 × 4	2.9579	4.3853	5.4058	7.4361	7.4361	12.903	12.903
	11 × 11 × 4	2.9558	4.3851	5.4054	7.4293	7.4293	12.901	12.901
	11 × 11 × 8	2.9524	4.3802	5.4018	7.4256	7.4256	12.898	12.898
	13 × 13 × 8	2.9514	4.3802	5.4016	7.4225	7.4225	12.897	12.897
	13 × 13 × 10	2.9513	4.3800	5.4015	7.4223	7.4223	12.897	12.897
0.2	9 × 9 × 4	2.7261	4.0298	4.9324	6.4506	6.4506	10.093	10.642
	11 × 11 × 4	2.7257	4.0297	4.9322	6.4492	6.4492	10.093	10.640
	11 × 11 × 8	2.7250	4.0287	4.9315	6.4485	6.4485	10.093	10.639
	13 × 13 × 8	2.7247	4.0286	4.9314	6.4479	6.4479	10.093	10.637
	13 × 13 × 10	2.7247	4.0286	4.9313	6.4478	6.4478	10.093	10.637
0.5	9 × 9 × 4	2.0442	2.8571	3.4668	3.9777	3.9777	4.0369	4.3056
	11 × 11 × 4	2.0442	2.8571	3.4667	3.9776	3.9776	4.0369	4.3055
	11 × 11 × 8	2.0441	2.8568	3.4665	3.9773	3.9773	4.0368	4.3053
	13 × 13 × 8	2.0440	2.8568	3.4665	3.9772	3.9772	4.0368	4.3052
	13 × 13 × 10	2.0440	2.8568	3.4664	3.9772	3.9772	4.0368	4.3052

Table 1. Convergence of frequency parameters of completely free FGM square plates with different thickness-to-width ratios h/b ($p = 1$).

As aforementioned, the boundary conditions can be easily obtained via changing the value of boundary springs. Therefore, the accuracy of the current method is strongly influenced by the values of springs' stiffness. To determine the appropriate values of spring's stiffness, the effects of elastic parameters on the frequencies of the FGM plate are investigated. The elastic parameter Γ is defined as ratios of corresponding spring's stiffness to bending stiffness $D_c = E_c h^3/12(1 - \mu_c^2)$. The plates are free at y = constant and restrained by only one kind of spring whose stiffness parameter ranges from 10^{-1} to 10^{10} at x = constant. The first three frequency parameters of the FGM square plates with $h/b = 0.2$ and $p = 1$ are presented in Table 2. It is obvious that the increase of the elastic parameter leads to increase of the frequency parameters. When $\Gamma \geq 10^7$, the influence of the elastic parameters on the frequencies of the plates can be neglected. The clamped boundary conditions can be simulated by assuming the elastic parameters equal to 10^9. The elastic boundary conditions can be obtained by assuming the elastic parameters equal to 100.

Γ	$k_u = \Gamma D,\ k_v = k_w = 0$			$K_v = \Gamma D,\ k_u = k_w = 0$			$K_w = \Gamma D,\ k_u = k_v = 0$		
	Ω_1	Ω_2	Ω_3	Ω_1	Ω_2	Ω_3	Ω_1	Ω_2	Ω_3
10^{-1}	0.0167	0.0464	0.0654	0.0167	0.0654	0.0802	0.0650	0.0654	0.1117
10^{0}	0.0419	0.1463	0.2069	0.0419	0.2069	0.2533	0.2028	0.2061	0.3514
10^{1}	0.1285	0.4615	0.6536	0.1286	0.6513	0.7985	0.6294	0.6301	1.1044
10^{2}	0.3984	1.4270	2.0440	0.3996	1.9750	2.4251	1.5056	1.7178	3.2905
10^{3}	1.0903	2.8583	3.7961	1.1184	3.0710	4.2125	2.0002	2.7732	5.9372
10^{4}	1.8471	3.1625	4.5503	2.0317	3.8426	4.3529	2.0785	3.0227	6.4327
10^{5}	2.0625	3.2758	4.5745	2.3675	4.2459	4.3815	2.0880	3.0600	6.5168
10^{6}	2.0904	3.2915	4.5774	2.4305	4.3436	4.3859	2.0891	3.0657	6.5299
10^{7}	2.0934	3.2932	4.5777	2.4464	4.3740	4.3870	2.0893	3.0664	6.5316
10^{8}	2.0937	3.2934	4.5778	2.4490	4.3790	4.3871	2.0893	3.0665	6.5318
10^{9}	2.0937	3.2934	4.5778	2.4493	4.3796	4.3871	2.0893	3.0665	6.5319
10^{10}	2.0937	3.2934	4.5778	2.4493	4.3796	4.3871	2.0893	3.0665	6.5319

Table 2. The first three frequency parameters Ω of the FGM square plates with different elastic parameters Γ (p=1).

3.1.2. Plate with general boundary conditions

To illustrate the accuracy of the present method, the comparisons of the current results with those in the published literature are presented. Table 3 presents the first two frequency parameters of the FGM square plates with different boundary conditions. The results are compared with those presented by Huang et al. [32] using the Ritz method on the basis of 3-D elasticity theory. Table 4 presents the fundamental frequency parameters of the FGM square plates with SSSS boundary conditions. Numerical vibration results for the same problems have been reported by Hosseini-Hashemi et al. [18] and Matsunaga [20] using HSDTs, showing that excellent agreement of the results is achieved.

	SSSS			CFFF			CFCF		
	Ref. []	**Present**	**Diff%**	**Ref. []**	**Present**	**Diff%**	**Ref. []**	**Present**	**Diff%**
Ω_1	3.406	3.406	0.000	0.6637	0.6657	0.347	3.400	3.421	0.618
Ω_2	6.296	6.296	0.000	1.432	1.434	0.140	3.820	3.840	0.524
Ω_3	6.296	6.296	0.000	2.154	2.158	0.186	5.774	5.787	0.225
Ω_4	7.347	7.345	0.027	3.396	3.405	0.265	5.976	5.989	0.218
Ω_5	7.347	7.345	0.027	4.347	4.348	0.023	7.609	7.657	0.631

Table 3. First five frequency parameters of FGM square plates with different boundary conditions (h/b = 0.2, p = 5).

http://dx.doi.org/10.5772/62335

h/b		*p = 0*	*p = 0.5*	*p = 1*	*p = 4*	*p = 10*	*p = ∞*
0.1	Ref. [18]	0.0577	0.0490	0.0443	0.0381	0.0364	0.0293
	Ref. [20]	0.0577	0.0492	0.0442	0.0381	0.0364	0.0293
	Present	0.0578	0.0491	0.0443	0.0381	0.0364	0.0294
0.2	Ref. [18]	0.2113	0.1807	0.1631	0.1378	0.1301	0.1076
	Ref. [20]	0.2121	0.1819	0.1640	0.1383	0.1306	0.1077
	Present	0.2122	0.1816	0.1640	0.1383	0.1306	0.1080

Table 4. Fundamental frequency parameters of FGM square plates with SSSS boundary conditions (a/b = 1).

BC	*h/b*	a/b = 1				a/b = 2			
		p = 0.6	*p = 1*	*p = 5*	*p = 10*	*p = 0.6*	*p = 1*	*p = 5*	*p = 10*
CSSS	0.1	5.660	5.235	4.434	4.272	12.66	11.71	10.01	9.671
	0.3	4.415	4.096	3.263	3.083	11.01	10.20	8.354	7.676
	0.5	3.391	3.156	2.435	2.265	6.866	6.464	5.023	4.591
CCSS	0.1	6.416	5.936	5.008	4.819	17.17	15.88	13.48	13.00
	0.3	4.807	4.464	3.520	3.313	13.68	12.69	10.12	9.566
	0.5	3.582	3.336	2.549	2.366	10.54	9.807	7.548	7.037
CCCS	0.1	7.437	6.884	5.772	5.544	17.71	16.38	13.90	13.40
	0.3	5.264	4.894	3.815	3.572	14.01	13.00	10.36	9.782
	0.5	3.797	3.540	2.681	2.479	10.75	10.00	7.679	7.153
CFFF	0.1	0.864	0.799	0.687	0.664	0.862	0.797	0.687	0.665
	0.3	0.816	0.755	0.637	0.613	0.845	0.781	0.669	0.647
	0.5	0.746	0.690	0.568	0.543	0.821	0.759	0.645	0.622
CCFF	0.1	1.684	1.558	1.330	1.285	4.230	3.911	3.356	3.246
	0.3	1.473	1.363	1.125	1.076	3.900	3.608	3.021	2.902
	0.5	1.253	1.160	0.932	0.885	3.479	3.220	2.627	2.506
CCCF	0.1	5.643	5.223	4.393	4.222	7.628	7.056	6.031	5.825
	0.3	4.074	3.785	2.956	2.774	6.594	6.107	5.009	4.781
	0.5	2.944	2.738	2.080	1.932	5.503	5.102	4.053	3.831

Table 5. Foundational frequency parameters Ω of FGM rectangular plates with different classical boundary conditions.

Several new numerical results for free vibration of FGM plates with general boundary conditions, including classical and elastic boundary conditions, are presented in Tables 5 and 6. The geometrical parameters are given as: a/b = 1 and 2, h/b = 0.1, 0.3 and 0.5. The different

boundary conditions, including CSSSS, CCSS, CCCS, CFFF, CCFF, CCCF, $E_1E_1E_1E_1$, $E_2E_2E_2E_2$ and $E_3E_3E_3E_3$, are studied. The power-law exponent is taken to be p = 0.6, 1, 5 and 10. From tables, it is obvious that the fundamental frequency of the plate strongly depends on the values of geometrical parameters, power-law index and boundary conditions. For the plates with classic boundary conditions, the foundational frequency parameters decrease with increase in the thickness-to-width ratio h/b. Except for plates with CFFF boundary conditions, the fundamental frequency parameters of the square plate (a/b = 1) are smaller than those of the plates with a/b = 2. The increase of the power-law index leads to decrease of the fundamental frequency parameter for all cases considered. For the plates with elastic restraints, the foundational frequency parameters increase as the length-to-width ratio a/b increases. Except for plates with h/b = 0.1 subjected to $E_2E_2E_2E_2$ and $E_3E_3E_3E_3$ boundary conditions, the foundational frequency parameters decrease with increase in the power-law index p. The effects of the thickness-to-width ratio h/b on the foundational frequency parameters are more complex. Some 3-D mode shapes for FGM plates with different boundary conditions are shown in Figs. 3 and 4.

BC	*h/b*	*a/b* = 1				*a/b* = 2			
		***p* = 0.6**	***p* = 1**	***p* = 5**	***p* = 10**	***p* = 0.6**	***p* = 1**	***p* = 5**	***p* = 10**
$E_1E_1E_1E_1$	0.1	4.798	4.437	3.786	3.655	12.138	11.228	9.626	9.303
	0.3	4.113	3.837	3.142	2.983	11.145	10.426	8.736	8.339
	0.5	3.444	3.236	2.522	2.352	10.019	9.439	7.495	7.035
$E_2E_2E_2E_2$	0.1	1.975	2.006	2.090	2.109	6.541	6.592	6.748	6.780
	0.3	3.043	3.025	2.844	2.773	9.601	9.476	8.804	8.569
	0.5	3.083	2.979	2.487	2.343	9.597	9.238	7.680	7.238
$E_3E_3E_3E_3$	0.1	1.823	1.823	1.828	1.826	5.690	5.649	5.586	5.563
	0.3	2.594	2.541	2.357	2.298	7.867	7.670	7.063	6.874
	0.5	2.724	2.634	2.234	2.123	8.308	8.014	6.799	6.471

Table 6. Foundational frequency parameters Ω of FGM rectangular plates with different elasticity boundary conditions.

3.2. Cylindrical shells

This section is concerned with the free vibration of FGM cylindrical shells with different boundary conditions. The convergence, accuracy and reliability of the present method are demonstrated by numerical examples and comparisons. New numerical results for the FGM cylindrical shells with the elastic boundary conditions are also presented. Unless stated otherwise the material properties for ceramic and metallic constituents of FGM cylindrical shells are given as follows: E_c = 168 GPa, μ_c = 0.3 and ρ_c = 5700 kg/m^3 and E_m = 70 GPa, μ_m = 0.3 and ρ_m = 2707 kg/m^3.

http://dx.doi.org/10.5772/62335

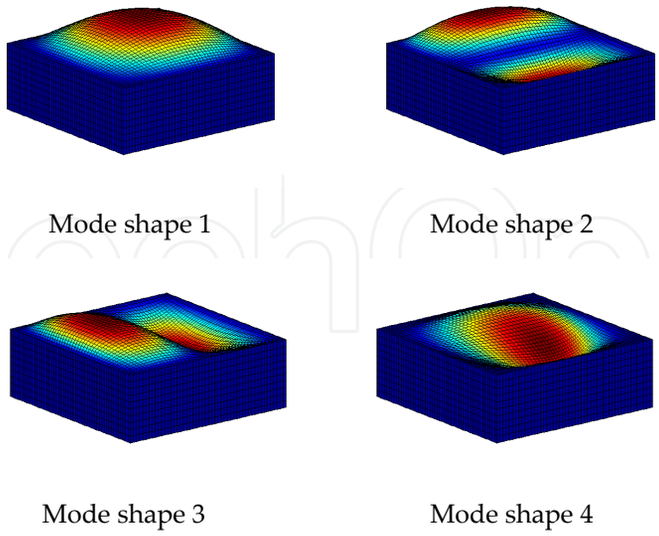

Figure 3. Mode shapes of FGM square plate with CCCC boundary conditions with $h/a = 0.5$ and $p = 1$.

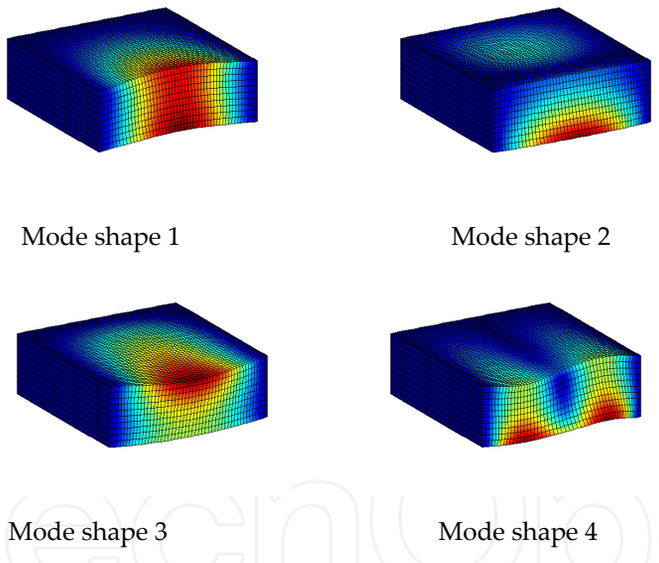

Figure 4. Mode shapes of FGM square plate with CCCF boundary conditions with $h/a = 0.5$ and $p = 1$.

3.2.1. Convergence study

The convergence studies of the first two frequencies for the completely free cylindrical shells with different circumferential wave numbers n are presented in Table 7. The different thickness-to-radius ratios (i.e., $h/R_0 = 0.1$, 0.2 and 0.5) and circumferential wave numbers (i.e., $n = 1$, 2, 3 and 4) are considered. The power-law exponent is taken to be $p = 1$. From Table 7, it is evident that the present method has a good convergence, and the truncated numbers of the displacement expressions will be uniformly selected as $M \times Q = 13 \times 13$.

h/R_0	$M \times Q$	$n = 1$		$n = 2$		$n = 3$		$n = 4$	
		f_1	f_2	f_1	f_2	f_1	f_2	f_1	f_2
0.1	10 × 10	675.95	775.84	72.216	93.963	202.45	236.49	383.66	422.39
	11 × 11	675.95	775.84	72.213	93.900	202.44	236.37	383.64	422.20
	12 × 12	675.95	775.82	72.211	93.898	202.43	236.36	383.61	422.19
	13 × 13	675.95	775.82	72.209	93.859	202.42	236.28	383.60	422.07
	14 × 14	675.95	775.81	72.208	93.858	202.42	236.28	383.58	422.06
0.2	10 × 10	702.69	829.15	156.06	195.32	426.43	484.16	782.43	843.50
	11 × 11	702.69	829.14	156.06	195.27	426.42	484.05	782.41	843.32
	12 × 12	702.69	829.12	156.05	195.27	426.41	484.04	782.37	843.29
	13 × 13	702.68	829.12	156.05	195.24	426.40	483.98	782.36	843.19
	14 × 14	702.68	829.11	156.05	195.24	426.39	483.97	782.34	843.18
0.5	10 × 10	813.89	990.82	472.71	513.27	1119.84	1157.84	1798.22	1821.60
	11 × 11	813.88	990.82	472.71	513.25	1119.82	1157.80	1798.18	1821.52
	12 × 12	813.88	990.81	472.70	513.25	1119.81	1157.78	1798.15	1821.49
	13 × 13	813.88	990.81	472.70	513.24	1119.80	1157.76	1798.13	1821.45
	14 × 14	813.88	990.81	472.70	513.24	1119.80	1157.75	1798.12	1821.43

Table 7. Convergence of the first two frequencies for the completely free cylindrical shells with different circumferential wave numbers n ($R_0 = 1$ m, $L/R_0 = 2$, $p = 1$).

Γ	$k_u = \Gamma D$, $k_v = k_w = 0$			$K_v = \Gamma D$, $k_u = k_w = 0$			$K_w = \Gamma D$, $k_u = k_v = 0$		
	$n = 1$	$n = 2$	$n = 3$	$n = 1$	$n = 2$	$n = 3$	$n = 1$	$n = 2$	$n = 3$
10^{-1}	6.0482	156.26	426.50	6.0495	156.10	426.42	6.3136	156.05	426.40
10^{0}	19.080	158.13	427.41	19.120	156.58	426.54	19.945	156.05	426.41
10^{1}	58.929	174.72	435.81	60.159	161.25	427.76	62.811	156.06	426.42
10^{2}	153.57	251.42	482.58	181.20	197.82	438.59	190.65	156.13	426.59
10^{3}	233.55	318.79	529.79	404.21	306.64	485.62	424.98	156.65	427.85
10^{4}	250.70	330.93	538.16	506.09	361.57	523.38	510.67	157.86	430.84
10^{5}	253.21	332.47	539.14	519.80	369.75	532.12	521.32	158.32	432.03
10^{6}	253.55	332.66	539.26	521.22	370.71	533.44	522.45	158.38	432.19
10^{7}	253.62	332.69	539.28	521.37	370.89	533.83	522.56	158.39	432.20
10^{8}	253.65	332.70	539.29	521.38	370.94	533.98	522.58	158.39	432.21

http://dx.doi.org/10.5772/62335

Γ	$k_u = \Gamma D,\ k_v = k_w = 0$			$K_v = \Gamma D,\ k_u = k_w = 0$			$K_w = \Gamma D,\ k_u = k_v = 0$		
	$n = 1$	$n = 2$	$n = 3$	$n = 1$	$n = 2$	$n = 3$	$n = 1$	$n = 2$	$n = 3$
10^9	253.66	332.71	539.29	521.38	370.95	534.00	522.58	158.39	432.21
10^{10}	253.66	332.71	539.29	521.38	370.95	534.00	522.58	158.39	432.21

Table 8. The frequencies of the FGM cylindrical shells with different elastic parameters Γ ($p = 1$).

It is significant to investigate the effects of elastic parameters on the frequencies of the cylindrical shells. The cylindrical shells are restrained by only one kind of spring whose stiffness parameter ranges from 10^{-1} to 10^{10} at x = constant. The frequencies of the cylindrical shells with different circumferential wave numbers n are presented in Table 8. The geometrical parameters are used as $R_0 = 1$ m, $L/R_0 = 2$ and $h/R_0 = 0.2$. The power-law index is taken to be $p = 1$. It is obvious that the increase of the elastic parameter leads to the increase of the frequency parameters. When $\Gamma \geq 10^7$, the influence of the elastic parameters on the frequencies of the plates can be neglected. The clamped boundary conditions can be simulated by assuming the elastic parameters equal to 10^9. The elastic boundary conditions can be obtained by assuming the elastic parameters equal to 100.

3.2.2. Cylindrical shells with general boundary conditions

To illustrate the accuracy of the present method, the comparisons of the current results with those in published literature are presented. Table 9 presents the first three frequency parameters $\lambda = \omega L \sqrt{\rho(1+\mu)/E}$ for the cylindrical shells with CC, CF and FF boundary conditions. The geometrical parameters are given as follows: $h/R = 0.3$, $L/R = 2$, $R = R_0 – R_i$. The results are compared with exact 3-D elasticity results by Malekzadeh et al. [31] using Layerwise theory and DQM (LW-DQ)and FEM. Table 10 presents first 10 frequencies of FGM cylindrical shells with CF boundary conditions. The geometrical parameters are given as follows: $R_i = 0.95$ m, R_0=1.05 m, $h = 0.1$ m, $L = 2$ m. Numerical vibration results of the same problems have been reported by Tornabene et al. [13] using FSDT and generalized DQM. It is noted that the V_c is defined as $V_c = (1–z/h)^p$. It is obvious that the results show very good agreement. The slight discrepancies may be due to the different solution strategies in the studies.

Several new numerical results for free vibration of FGM cylindrical shells with general boundary conditions, including classical and elastic boundary conditions, are presented in Tables 11 and 12. The geometrical parameters are given as follows: $R_0 = 1$ m, $L/R_0 = 2$, h/R_0 = 0.1, 0.3 and 0.5. The different boundary conditions, including CC, CS, SS, CF, SF, E_1E_1, E_2E_2 and E_3E_3, are studied. The power-law exponent is taken to be p = 0, 0.6, 1, 2, 5, 10 and 20. It is observed from Table 11 that the boundary conditions have a significant effect on the frequencies of cylindrical shells. The higher constraints at edges may increase the flexural rigidity of the shell leading to higher frequency response. It is obvious that the increase of the thickness-to-radius ratio h/R_0 leads to the increase of the frequency parameters. It is also seen that the fundamental frequencies decrease as the power-law index increases. From Table 12, the frequencies of shells also increase as thickness-to-radius ratio h/R_0 increases. However, the effects of the power-law index on the frequencies of shells became more complex. Some 3-D mode shapes for FGM cylindrical shells with different boundary conditions are shown in Figs. 5 and 6.

BC	*n*	λ_1			λ_2			λ_3		
		LW-DQ [31]	**FEM [31]**	**Present**	**LW-DQ [31]**	**FEM [31]**	**Present**	**LW-DQ [31]**	**FEM [31]**	**Present**
CC	1	1.7860	1.7972	1.7905	2.6043	2.6222	2.6050	3.4148	3.4192	3.4245
	2	1.7452	1.7573	1.7500	3.2942	3.3114	3.2949	3.4921	3.5150	3.5012
	3	1.8867	1.8862	1.8912	3.6024	3.6320	3.6099	3.9416	3.9257	3.9447
	4	2.1966	2.2072	2.2004	3.8126	3.8228	3.8193	4.2757	4.3215	4.2783
	5	2.6385	2.6617	2.6415	4.1302	4.1327	4.1364	4.7010	4.7322	4.7031
CF	1	0.7514	0.7546	0.7516	1.7563	1.7692	1.7568	1.8800	1.8996	1.8812
	2	0.6620	0.6713	0.6622	1.8962	1.9256	1.8980	2.1305	2.1557	2.1324
	3	0.9246	0.9301	0.9247	2.0610	2.0668	2.0630	2.5165	2.5482	2.5179
	4	1.4021	1.4282	1.4021	2.4030	2.4646	2.4049	2.9919	3.0342	2.9930
	5	1.9814	2.0228	1.9814	2.8666	2.8571	2.8684	3.5251	3.5628	3.5258
FF	1	0.0000	0.0000	0.0000	0.0001	0.0001	0.0003	1.0710	1.0734	1.0709
	2	0.2576	0.2608	0.2576	0.3800	0.3831	0.3799	1.3533	1.3594	1.3532
	3	0.6884	0.6890	0.6884	0.9253	0.9377	0.9252	1.8689	1.8794	1.8689
	4	1.2302	1.2525	1.2302	1.5160	1.5307	1.5158	2.4754	2.4917	2.4753
	5	1.8427	1.8694	1.8426	2.1343	2.1532	2.1341	3.1169	3.1417	3.1169

Table 9. First three frequency parameters of the cylindrical shells with different boundary conditions ($\mu = 0.3$).

	p = 0		**p = 0.6**		**p = 1**		**p = 5**	
	Ref. [13]	**Present**	**Ref. [13]**	**Present**	**Ref. [13]**	**Present**	**Ref. [13]**	**Present**
f_1	152.93	152.13	150.03	148.67	149.29	147.76	148.75	147.10
f_2	152.93	152.13	150.03	148.67	149.29	147.76	148.75	147.10
f_3	220.06	219.31	212.94	211.89	212.22	211.00	219.49	218.00
f_4	220.06	219.31	212.94	211.89	212.22	211.00	219.49	218.00
f_5	253.78	254.30	250.74	250.36	249.31	248.68	243.43	242.86
f_6	253.78	254.30	250.74	250.36	249.31	248.68	243.43	242.86
f_7	383.55	384.04	370.63	370.69	369.46	369.21	383.71	382.79
f_8	383.55	384.04	370.63	370.69	369.46	369.21	383.71	382.79
f_9	420.51	420.86	415.47	414.68	412.97	411.88	402.56	401.57
f_{10}	431.45	428.75	420.39	416.91	418.46	414.66	423.57	419.16

Table 10. First 10 frequencies (Hz) of the FGM cylindrical shells with F–C boundary conditions.

http://dx.doi.org/10.5772/62335

BC	h/R_0	$p = 0$	$p = 0.6$	$p = 1$	$p = 2$	$p = 5$	$p = 10$	$p = 20$
CC	0.1	390.33	377.23	374.78	375.39	379.94	379.62	376.24
	0.3	621.15	599.34	594.11	591.68	594.96	595.70	593.23
	0.5	701.10	686.38	681.10	674.46	668.80	666.26	663.96
CS	0.1	378.25	365.82	363.43	363.82	367.81	367.48	364.19
	0.3	567.55	548.06	543.23	540.49	542.33	542.55	540.43
	0.5	648.20	634.72	629.77	623.22	617.07	614.23	612.09
SS	0.1	367.68	355.76	353.44	353.68	357.26	356.85	353.71
	0.3	528.69	510.67	506.15	503.35	504.53	504.51	502.59
	0.5	608.85	596.84	592.29	585.94	579.40	576.22	574.05
CF	0.1	153.27	149.63	148.75	148.30	148.46	147.80	146.56
	0.3	257.65	254.87	253.62	251.58	248.56	246.32	244.47
	0.5	263.06	261.04	260.07	258.44	255.66	253.17	250.86
SF	0.1	149.92	146.38	145.51	145.06	145.17	144.51	143.30
	0.3	247.41	245.02	243.86	241.81	238.61	236.30	234.48
	0.5	248.50	246.92	246.06	244.45	241.51	238.95	236.67

Table 11. Fundamental frequencies of FGM cylindrical shells with different classical boundary conditions.

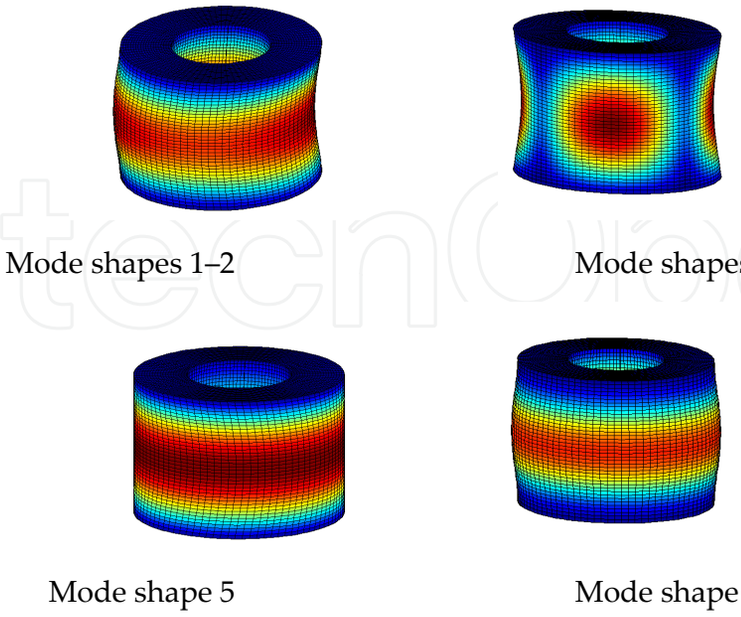

Figure 5. Mode shapes of FGM cylindrical shells with CC boundary conditions with $h/R_0 = 0.5$, $L/R_0 = 2$ and p=1.

BC	h/R_0	$p = 0$	$p = 0.6$	$p = 1$	$p = 2$	$p = 5$	$p = 10$	$p = 20$
E_1E_1	0.1	368.31	356.53	354.28	354.66	358.44	358.13	355.04
	0.3	558.81	545.07	542.41	542.83	548.35	550.42	549.32
	0.5	669.03	660.42	657.10	652.86	649.27	647.64	645.98
E_2E_2	0.1	82.564	91.860	95.778	101.94	109.61	113.78	116.41
	0.3	381.14	384.20	386.62	392.04	400.91	405.96	408.78
	0.5	539.57	539.80	540.83	544.12	551.17	556.07	559.18
E_3E_3	0.1	80.874	89.444	93.013	98.592	105.46	109.13	111.41
	0.3	331.30	347.67	354.18	364.51	377.62	384.51	388.49
	0.5	515.44	522.81	525.80	531.29	539.88	545.19	548.45

Table 12. Fundamental frequencies of FGM cylindrical shells with different elasticity boundary conditions.

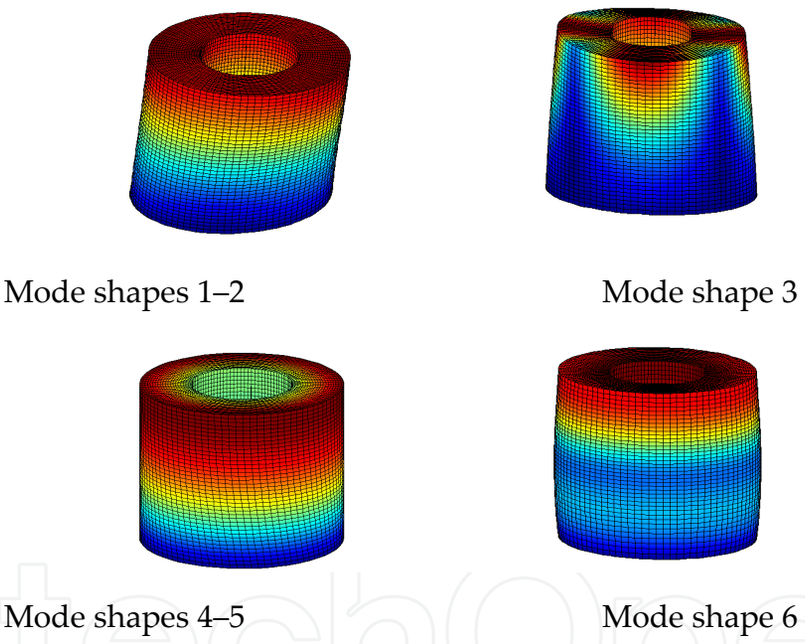

Figure 6. Mode shapes of FGM cylindrical shells with CF boundary conditions with $h/R_0 = 0.5$, $L/R_0 = 2$ and $p = 1$.

4. Conclusions

A new 3-D exact solution for free vibration analysis of thick functionally graded plates and cylindrical shells with arbitrary boundary conditions is presented in this chapter. The effective material properties of functionally graded structures vary continuously in the thickness direction according to the simple power-law distributions in terms of volume fraction of constituents and are estimated by Voigt's rule of mixture. By using the artificial spring

boundary technique, the general boundary conditions can be obtained by setting proper spring stiffness. All displacements of the functionally graded plates and shells are expanded in the form of the linear superposition of standard 3-D cosine series and several supplementary functions, which are introduced to remove potential discontinuity problems with the original displacements along the edge. The Rayleigh-Ritz procedure is used to yield the accurate solutions. The convergence, accuracy and reliability of this formulation are verified by numerical examples and by comparng the current results with those in published literature. The influence of the geometrical parameters and elastic foundation on the frequencies of rectangular plates and cylindrical shells is investigated.

Acknowledgements

The authors gratefully acknowledge the financial support from the National Natural Science Foundation of China (Nos. 51175098 and 51279035) and the Fundamental Research Funds for the Central Universities of China (No. HEUCFQ1401).

Author details

Guoyong Jin, Zhu Su* and Tiangui Ye

*Address all correspondence to: xiuzhu0403@163.com

College of Power and Energy Engineering, Harbin Engineering University, Harbin, P.R. China

References

[1] Zhang D., Zhou Y. A theoretical analysis of FGM thin plates based on physical neutral surface. Computational Material Science. 2008; 44: 716–20.

[2] Chi S., Chung Y. Mechanical behavior of functionally graded material plates under transverse load – Part ◎: Analysis. International Journal of Solids and Structures. 2006; 43: 3657–74.

[3] Chi S., Chung Y. Mechanical behavior of functionally graded material plates under transverse load – Part ◎: Numerical results. International Journal of Solids and Structures. 2006; 43: 3675–91.

[4] Latifi M., Farhatnia F., Kadkhodaei M. Bucking analysis of rectangular functionally graded plates under various edge conditions using Fourier series expansion. European Journal of Mechanics – A/Solids. 2013; 41: 16–27.

[5] Zhao X., Lee Y.Y., Liew K.M. Free vibration analysis of functionally graded plates using the element-free kp-Ritz method. Journal of Sound and Vibration. 2009; 319: 918–39.

[6] Hosseini-Hashemi S., Rokni Damavandi Taher H., Akhavan H., Omidi M. Free vibration of functionally graded rectangular plates using first-order shear deformation plate theory. Applied Mathematical Modelling. 2010; 34: 1276–91.

[7] Hosseini-Hashemi S., Fadaee M., Atashipour S.R. A new exact analytical approach for free vibration of Reissner-Mindlin functionally graded rectangular plates. International Journal of Mechanical Sciences. 2011; 53: 11–22.

[8] Ferreira A.J.M., Batra R.C., Roque C.M.C., Qian L.F., Jorge R.M.N. Natural frequencies of functionally graded plates by a meshless method. Composite Structures. 2006; 75: 593–600.

[9] Fallah A., Aghdam M.M., Kargarnovin M.H. Free vibration analysis of moderately thick functionally graded plates on elastic foundation using extended Kantorovich method. Archive of Applied Mechanics. 2013; 83: 177–91.

[10] Croce L.D., Venini P. Finite elements for functionally graded Reissner-Mindlin plates. Compute Methods in Applied Mechanics and Engineering. 2004; 193: 705–25.

[11] Kadoli R., Ganesan N. Buckling and free vibration analysis of functionally graded cylindrical shells subjected to a temperature-specified boundary condition. Journal of Sound and Vibration. 2006; 289(3): 450–80.

[12] Tornabene F. Free vibration analysis of functionally graded conical, cylindrical shell and annular plate structures with a four-parameter power-law distribution. Computer Methods in Applied Mechanics and Engineering. 2009; 198(37): 2911–35.

[13] Tornabene F., Viola E., Inman D.J. 2-D differential quadrature solution for vibration analysis of functionally graded conical, cylindrical shell and annular plate structures. Journal of Sound and Vibration. 2009; 328(3): 259–90.

[14] Sheng G.G., Wang X. Thermomechanical vibration analysis of a functionally graded shell with flowing fluid. European Journal of Mechanics – A/Solids. 2008; 27(6): 1075–87.

[15] Jin G.Y., Xie X., Liu Z.G. The Haar wavelet method for free vibration analysis of functionally graded cylindrical shells based on the shear deformation theory. Composite Structures. 2014; 108: 435–48.

[16] Qu Y.G., Long X.H., Yuan G.Q., Meng G. A unified formulation for vibration analysis of functionally graded shells of revolution with arbitrary boundary conditions. Composites Part B: Engineering. 2013; 50: 381–402.

[17] Reddy J.N. Analysis of functionally graded plates. International Journal of Numerical Methods in Engineering. 2000; 47: 663–84.

[18] Hosseini-Hashemi S., Fadaee M., Atashipour S.R. Study on the free vibration of thick functionally graded rectangular plates according to a new exact closed-form procedure. Composite Structures. 2011; 93: 722–35.

[19] Baferani A.H., Saidi A.R., Ehteshami H. Accurate solution for free vibration analysis of functionally graded thick rectangular plates resting on elastic foundation. Composite Structures. 2011; 93: 1842–53.

[20] Matsunaga H. Free vibration and stability of functionally graded plates according to a 2-D higher-order deformation theory. Composite Structures. 2008; 82: 499–512.

[21] Ferreira A.J.M., Batra R.C., Roque C.M.C., Qian L.F., Martins P.A.L.S. Static analysis of functionally graded plates using third-order shear deformation theory and a meshless method. Composite Structures. 2005; 69: 449–57.

[22] Qian L.F., Batra R.C., Chen L.M. Static and dynamic deformations of thick functionally graded elastic plates by using higher-order shear and normal deformable plate theory and meshless local Petrov-Galerkin method. Composites Part B: Engineering. 2004; 35: 685–97.

[23] Najafizadeh M.M., Isvandzibaei M.R. Vibration of functionally graded cylindrical shells based on higher order shear deformation plate theory with ring support. Acta Mechanica. 2007; 191(1–2): 75–91.

[24] Matsunaga H. Free vibration and stability of functionally graded circular cylindrical shells according to a 2D higher-order deformation theory. Composite Structures. 2009; 88(4): 519–31.

[25] Viola E., Rossetti L., Fantuzzi N. Numerical investigation of functionally graded cylindrical shells and panels using the generalized unconstrained third order theory coupled with the stress recovery. Composite Structures. 2012; 94(12): 3736–58.

[26] Zozulya V.V., Zhang C. A high order theory for functionally graded axisymmetric cylindrical shells. International Journal of Mechanical Sciences. 2012; 60(1): 12–22.

[27] Vel S.S., Batra R.C. Three-dimensional exact solution for the vibration of functionally graded rectangular plates. Journal of Sound and Vibration. 2004; 272: 703–30.

[28] Reddy J.N., Cheng Z.Q. Three-dimensional thermoelastic deformations of a functionally graded elliptic plate. Composites Part B: Engineering. 2000; 31: 97–106.

[29] Amini M.H., Soleimani M., Rastgoo A. Three-dimensional free vibration analysis of functionally graded material plates resting on an elastic foundation. Smart Materials and Structure. 2009; 18: 1–9.

[30] Malekzadeh P. Three-dimensional free vibration analysis of thick functionally graded plates on elastic foundations. Composite Structures. 2009; 89: 367–73.

[31] Malekzadeha P., Faridb M., Zahedinejadc P., Karamid G. Three-dimensional free vibration analysis of thick cylindrical shells resting on two-parameter elastic supports. Journal of Sound and Vibration. 2008; 313: 655–75.

[32] Huang C.S., Yang P.J., Chang M.J. Three-dimensional vibration analyses of functionally graded material rectangular plates with through internal cracks. Composite Structures. 2012; 94(9): 2764–76.

[33] Santos H., Mota Soares C.M., Mota Soares C.A., Reddy J.N. A semi-analytical finite element model for the analysis of cylindrical shells made of functionally graded materials. Composite Structures. 2009; 91(4): 427–32.

[34] Qu Y.G., Meng G. Three-dimensional elasticity solution for vibration analysis of functionally graded hollow and solid bodies of revolution. Part I: Theory. European Journal of Mechanics – A/Solids. 2014; 44: 222–33.

[35] Qu Y.G., Meng G. Three-dimensional elasticity solution for vibration analysis of functionally graded hollow and solid bodies of revolution. Part II: Application. European Journal of Mechanics – A/Solids. 2014; 44: 234–48.

[36] Saada A.S. Elasticity: Theory and applications. 2nd ed. Florida: Ross Publishing, Inc; 2009.

[37] Shen H.S. Functionally graded materials: Nonlinear analysis of plates and shells. Florida: CRC Press; 2009.

[38] Li W.L. Vibration analysis of rectangular plates with general elastic boundary supports. Journal of Sound and Vibration. 2004; 273(3): 619–35.

[39] Beslin O., Nicolas J. A hierarchical functions set for predicting very high order plate bending modes with any boundary conditions. Journal of Sound and Vibration. 1997; 202(5): 633–55.

[40] Ye T.G., Jin G.Y., Shi S.X., Ma X.L. Three-dimensional free vibration analysis of thick cylindrical shells with general end conditions and resting on elastic foundations. International Journal of Mechanical Sciences. 2014; 84: 120–37.

[41] Jin G.Y., Su Z., Shi S.X., Ye T.G., Gao S.Y. Three-dimensional exact solution for the free vibration of arbitrarily thick functionally graded rectangular plates with general boundary conditions. Composite Structures. 2014; 108: 565–77.

[42] Su Z., Jin G.Y., Ye T.G. Three-dimensional vibration analysis of thick functionally graded conical, cylindrical shell and annular plate structures with arbitrary elastic restraints. Composite Structures. 2014; 118: 432–47.

[43] Jin G.Y., Su Z., Ye T.G., Jia X.Z. Three-dimensional vibration analysis of isotropic and orthotropic conical shells with elastic boundary restraints. International Journal of Mechanical Sciences. 2014; 89: 207–21.